

Communication

Mechanical Properties and Photomechanical Fatigue of Macro- and Nano-dimensional Diarylethene Molecular Crystals

Thiranjeeva I. Lansakara, Fei Tong, Christopher J. Bardeen, and Alexei V. Tivanski

Nano Lett., **Just Accepted Manuscript** • DOI: 10.1021/acs.nanolett.0c02631 • Publication Date (Web): 21 Aug 2020

Downloaded from pubs.acs.org on August 22, 2020

Just Accepted

“Just Accepted” manuscripts have been peer-reviewed and accepted for publication. They are posted online prior to technical editing, formatting for publication and author proofing. The American Chemical Society provides “Just Accepted” as a service to the research community to expedite the dissemination of scientific material as soon as possible after acceptance. “Just Accepted” manuscripts appear in full in PDF format accompanied by an HTML abstract. “Just Accepted” manuscripts have been fully peer reviewed, but should not be considered the official version of record. They are citable by the Digital Object Identifier (DOI®). “Just Accepted” is an optional service offered to authors. Therefore, the “Just Accepted” Web site may not include all articles that will be published in the journal. After a manuscript is technically edited and formatted, it will be removed from the “Just Accepted” Web site and published as an ASAP article. Note that technical editing may introduce minor changes to the manuscript text and/or graphics which could affect content, and all legal disclaimers and ethical guidelines that apply to the journal pertain. ACS cannot be held responsible for errors or consequences arising from the use of information contained in these “Just Accepted” manuscripts.

1
2
3
4
5
6
7
8
9
10
11
12
13
14
15
16
17
18
19
20
21
22
23
24
25
26
27
28
29
30
31
32
33
34
35
36
37
38
39
40
41
42
43
44
45
46
47
48
49
50
51
52
53
54
55
56
57
58
59
60

Mechanical Properties and Photomechanical Fatigue of Macro- and Nano-dimensional Diarylethene Molecular Crystals

Thiranjeeva I. Lansakara[†], Fei Tong[‡], Christopher J. Bardeen^{ ‡}, Alexei V. Tivanski^{* †}*

[†]Department of Chemistry, The University of Iowa, Iowa City, Iowa 52242, United States

[‡]Department of Chemistry, University of California Riverside, Riverside, California 92521,
United States

KEYWORDS: AFM nanoindentation, photomechanical fatigue, photo reversible,

molecular crystals, nanowires, Young's modulus

ABSTRACT

The diarylethene derivative, 1,2-bis(2,4-dimethyl-5-phenyl-3-thienyl)perfluorocyclopentene undergoes a reversible photoisomerization between its

1
2
3 ring-open and ring-closed forms in the solid-state and has applications as a
4
5
6
7 photomechanical material. Mechanical properties of macro-crystals, nanowire single
8
9
10 crystals and amorphous films as a function of multiple sequential UV and visible light
11
12
13 exposures have been quantified using atomic force microscopy nanoindentation. The
14
15
16 isomerization reaction has no effect on the elastic modulus of each solid. But going from
17
18
19 the macro- to the nanowire crystal results in a remarkable over threefold decrease in the
20
21
22 elastic modulus. The macro-crystal and amorphous solids are highly resistant to
23
24
25 photomechanical fatigue, while nanowire crystals show clear evidence of
26
27
28 photomechanical fatigue attributed to a transition from crystal to amorphous forms. This
29
30
31 study provides first experimental evidence of size dependent photomechanical fatigue in
32
33
34 photoreactive molecular crystalline solids and suggests crystal morphology and size must
35
36
37 be considered for future photomechanical applications.
38
39
40
41
42
43
44
45
46

47 INTRODUCTION

48
49
50

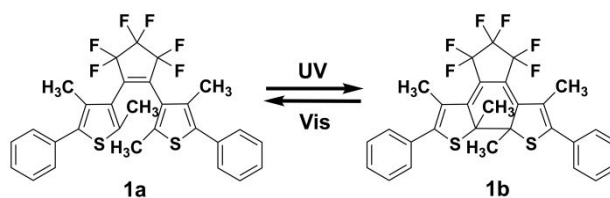
51 Photochemical reactions that occur in the solid crystalline state can be utilized for direct
52
53
54 conversion of light energy to macroscopic anisotropic movements of the solid.¹⁻² The
55
56
57
58
59
60

1
2
3 strain built up between the reactant and product crystal phases results in a variety of
4
5
6
7 exciting macroscopic mechanical shape behaviors including bending,³ twisting,⁴
8
9
10 expansion,⁵ contraction,⁶ fragmentation,⁷ and coiling.⁸ Recently, several examples of
11
12
13 photochemical reactions that led to mechanical motions of solids were reported, including
14
15
16 E-Z photoisomerization,⁹⁻¹⁰ [2+2]¹¹ and [4+4]^{5, 12} photodimerization, linkage
17
18 isomerization¹³ and ring opening – closing isomerization.¹⁴⁻¹⁶ Development of
19
20
21 photomechanical molecular crystals may enable the creation of actuators that allow facile
22
23
24 conversion of light energy into mechanical work.
25
26
27
28
29
30

31 Diarylethenes are a class of photochromic molecules that undergo a reversible ring
32
33 opening – ring closing photoisomerization as a result of exposure to visible and ultraviolet
34
35 (UV) light (Scheme 1). Both isomers are thermally stable with relatively fast conversion
36
37
38 times, and the solids show high resistance to photomechanical fatigue.¹⁷⁻²¹ In order to
39
40
41 reduce the probability of fracture during photoreaction, nanoscale crystals and
42
43
44 composites are often used.²²⁻²⁴ For example, 1,2-bis(2,4-dimethyl-5-phenyl-3-
45
46
47 thienyl)perfluorocyclopentene (DAE) crystalline nanowires with ~200 nm diameter have
48
49
50
51
52
53
54
55
56
57
58
59
60

1
2
3
4 been utilized to generate reversible photomechanical motion.²³ Furthermore, a
5
6
7 macroscopic actuator based on DAE derivative nanowires embedded into a template was
8
9
10 utilized to reversibly lift an object approximately 10^4 times its own weight.²⁵ However,
11
12
13
14 beyond 50 cycles, evidence of photomechanical fatigue appeared, which was tentatively
15
16
17 attributed to molecular interactions between the template walls and DAE nanowires. In
18
19
20
21 contrast, bulk macro-crystals and solutions of DAE showed high stability after more than
22
23
24
25 500 cycles.

30
31 **Scheme 1.** Photochemical interconversion between ring-open (1a) and ring-closed (1b)
32
33
34 isomers with UV (~360 nm) and visible (~530 nm) light exposures.



50
51 Photomechanical fatigue is a common issue that hinders the development of materials
52
53
54 based on organic photochromism, including photomechanical actuators and optical
55
56
57
58
59
60

1
2
3 memories.^{12, 26} It is generally attributed to a combination of chemical side reactions and
4
5
6
7 irreversible structural changes in the solid such as defect accumulation and fracture.²⁷
8
9

10 But the **DAE** results suggest that there is a large difference in the fatigue resistance of
11
12
13
14 nanowires versus macro-crystals. While the effect of nanosizing on the electrical
15
16
17 properties of semiconductors is reasonably well understood, how morphology at the
18
19
20
21 nanoscale affects mechanical properties of crystalline solids is poorly understood,
22
23
24 especially for organic materials²⁸⁻³¹ that are typically softer than inorganic solids.³²
25
26
27

28 Although photomechanical motion and photomechanical fatigue are largely governed by
29
30
31 the elastic properties of photomechanical molecular solids,²⁷ studies of the mechanical
32
33
34 properties of such solids are scarce.³³
35
36
37

38 Herein, we elucidate the origin of the photomechanical fatigue observed in the **DAE**
39
40
41 crystalline nanowires. Atomic force microscopy (AFM) nanoindentation is used to
42
43
44
45 measure the elastic modulus (Young's modulus) of solid **DAE** samples with different
46
47
48 morphologies: individual macro-crystals, nanowire single crystals and amorphous films.
49
50
51
52 These samples are interconverted between the ring-open (**1a**) and ring-closed (**1b**) forms
53
54
55
56
57
58
59
60

1
2
3 using alternating UV and visible light exposures. We demonstrate the mechanical
4
5
6 properties of the two isomers are similar yet vary depending on the crystal morphology
7
8
9 and size. Evidence of the photomechanical fatigue is observed by quantifying a decrease
10
11
12 in the Young's modulus of a **DAE** individual nanowire as a result of repeated UV and
13
14
15 visible light exposures. The origin of the photomechanical fatigue is attributed to a
16
17
18 transition from crystal to amorphous forms in the nanowires.
19
20
21
22
23
24
25
26
27

28 RESULTS AND DISCUSSION

29
30
31
32

33 Figure 1 shows representative AFM 3D height images of each **DAE** sample after visible
34
35 (~532 nm) and then UV (~360 nm) light exposure. The solid samples underwent a clear
36
37
38 change in color, from colorless ring-open isomer **1a** to blue-colored ring-closed isomer **1b**
39
40
41 after the UV exposure and then back to colorless **1a** isomer after the visible light
42
43
44 exposure. The macro-crystal surface was reasonably flat with 15 – 30 nm tall rounded
45
46
47 features spread across the crystal surface, as also observed for other molecular macro-
48
49
50 crystals.^{28, 34} The nanowires were 2 – 4 μm long and 180 ± 20 nm in diameter, lying flat
51
52
53
54
55
56
57
58
59
60

1
2
3 on the AAO template surface with features ranging in 20 – 80 nm in height (Figure 1b).

4
5
6
7 The amorphous film was significantly smoother (Figure 1c) compared to both macro-
8
9
10 crystal and nanowire samples. None of the solids exhibited a change in localized AFM-
11
12
13 determined sample topography as a result of photoirradiation (root-mean-square
14
15
16 roughness for each solid before and after light exposure is reported in Table S1). This is
17
18
19
20 consistent with the relatively small change in molecular geometry upon isomerization,
21
22
23 with only ~10% expected shortening of the distance between 5- and 5' carbons in the two
24
25
26
27 thiophene rings.¹⁷ Large-scale mechanical motion of the nanowires (e.g. bending) was
28
29
30
31 prevented by adhesion to the dry AAO template surface.
32
33
34
35
36
37
38
39
40
41
42
43
44
45
46
47
48
49
50
51
52
53
54
55
56
57
58
59
60

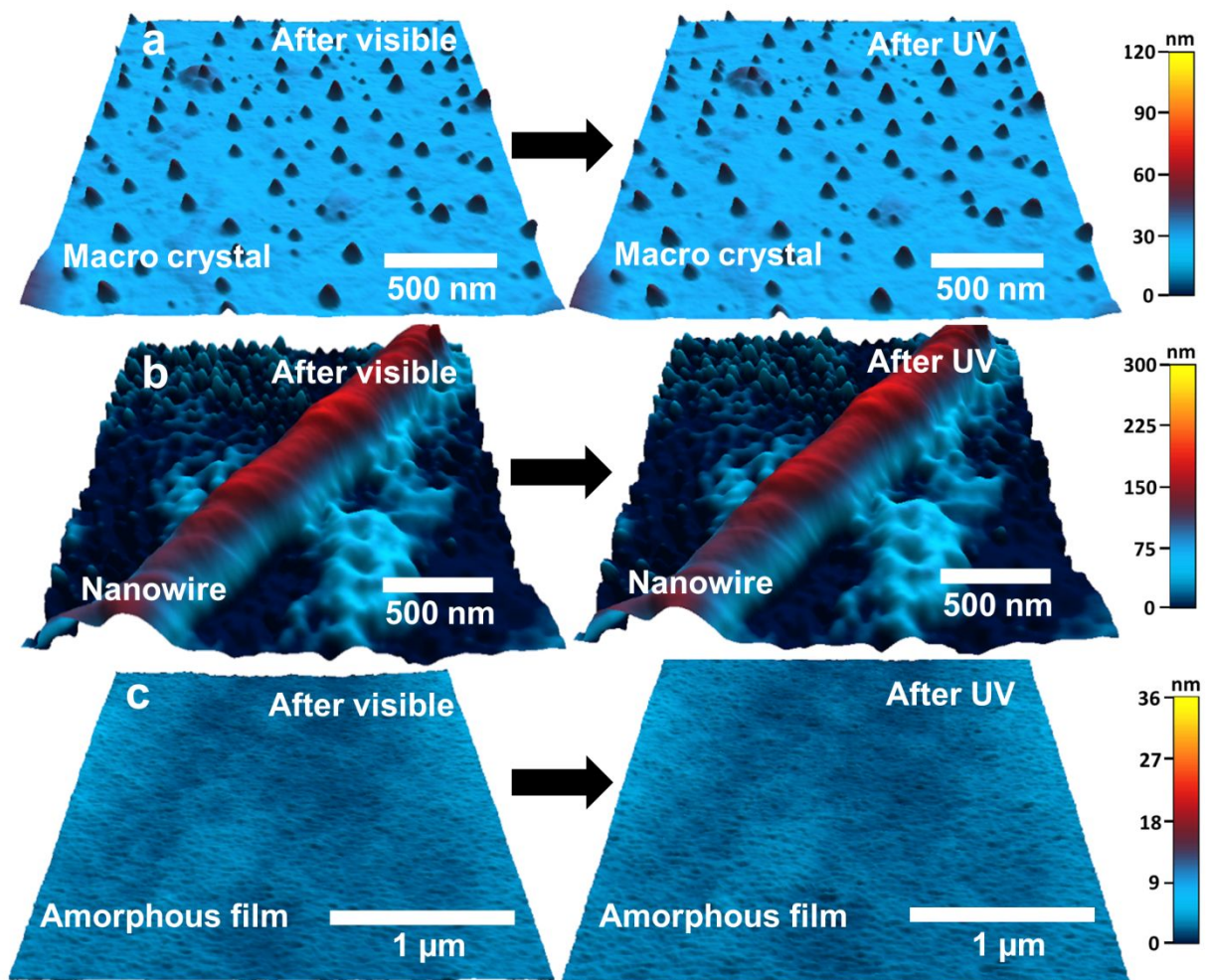
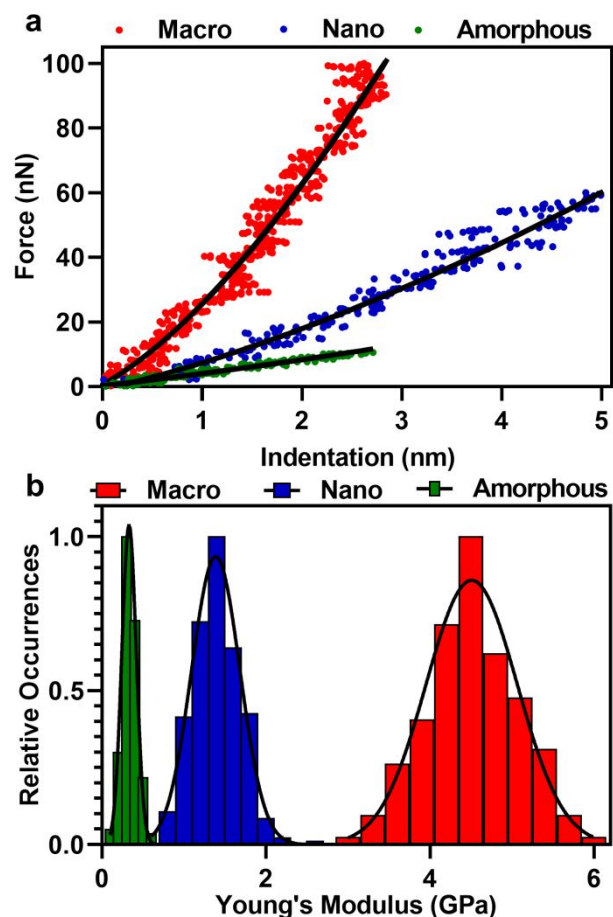


Figure 1. Representative AFM 3D height images of DAE (a) macro-crystal, (b) nanowire single crystal, and (c) amorphous film after visible (left) and UV (right) light exposure. No change in the localized sample topography for each solid was observed as a result of one cycle with visible and UV light exposures.

AFM nanoindentation measurements were carried out after first exposing each solid to visible light to ensure the DAE was initially in the 1a isomer. Representative force versus

1
2
3 indentation distance curves are shown in Figure 2a. Young's modulus values were
4
5
6
7 determined by fitting the approach force data to the JKR elastic contact model. Averaged
8
9
10 Young's moduli for each solid at different sample positions were within one standard
11
12
13 deviation of each other, enabling us to combine the values from all sample positions for
14
15
16
17 each solid to a single histogram (Figure 2b). The resultant histogram for each sample was
18
19
20
21 fit using a Gaussian function to determine the most probable Young's modulus and
22
23
24 corresponding standard deviation.
25
26
27



1
2
3
4
5
6
7 **Figure 2.** (a) Representative force curves collected on **DAE** macro crystal (red), nanowire
8 (blue), and amorphous film (green). Solid black lines are the JKR fit. (b) Histograms of
9
10
11 Young's moduli for the **DAE** macro (red), nanowire (blue) and amorphous film(green).
12
13
14
15
16
17
18 Solid black lines are Gaussian fits.

19
20
21
22
23
24
25 The most probable Young's moduli for **1a** single macro-crystal, nanowire single crystal
26
27
28 and amorphous film were 4.4 ± 0.4 GPa, 1.4 ± 0.1 GPa and 0.34 ± 0.04 GPa, respectively.

29
30
31 After the samples were exposed to UV light to yield **1b** isomer, macro-crystal undergoes
32
33
34
35 photo-induced movement which was absent for the substrate-deposited nanowire and
36
37
38 amorphous film. The AFM nanoindentation measurements before and after light
39
40
41
42 exposures were performed on the macro-crystal over a similar $5 \mu\text{m} \times 5 \mu\text{m}$ sample region
43
44
45
46 which was located using AFM imaging and top-view optical camera. AFM nanoindentation
47
48
49 measurements were performed on similar sample positions for the **DAE** nanowire and
50
51
52 amorphous film samples. The most probable Young's moduli for **1b** single macro-crystal,
53
54
55
56
57
58
59
60

1
2
3 nanowire single crystal and amorphous film were 4.5 ± 0.5 GPa, 1.3 ± 0.15 GPa and 0.35
4
5
6
7 ± 0.03 GPa, respectively. Since the most probable Young's moduli for the two isomers
8
9
10 for each sample were statistically similar, the Young's moduli values for the ring-open and
11
12
13 ring-closed isomers were combined into a single histogram for each sample. Figure 2b
14
15
16 displays the combined Young's moduli histogram of single macro-crystal (red), nanowire
17
18 single crystal (blue) and amorphous film (green) with the Gaussian fits (black). We note
19
20
21 that the similar elastic moduli for the two isomers and absence of localized sample
22
23
24 topography changes, is consistent with the relatively small change in molecular geometry
25
26
27 upon isomerization. Irie and coworkers previously showed that the **DAE** macro-crystals
28
29
30 undergo single-crystal to single-crystal photoisomerization with each cycle of the UV and
31
32
33 visible light exposure.³⁵ The degree of **DAE 1a** to **1b** conversion efficiency is dependent
34
35
36 on the photostationary state and solid sample thickness as a result of a positive
37
38
39 photochrome formation.³⁶⁻³⁷ For amorphous film and macro-crystal solids, the expected
40
41
42 conversion efficiencies from **1a** to **1b** are 5-10%, similar to 6% conversion observed for a
43
44
45
46
47
48
49
50
51
52
53
54
55
56
57
58
59
60
50 μm thick **DAE** sample.²⁵ For individual nanowires with thicknesses less than 200 nm,

1
2
3 the expected conversion efficiency will likely be closer to 79% observed for the DAE
4
5
6
7 molecules in a hexane solution.³⁸
8
9

10 The Young's modulus of the **DAE** amorphous film (0.35 GPa) is comparable to low-
11
12
13
14 density polyethylene (0.20 – 0.30 GPa).³⁹ The Young's modulus of **DAE** single macro-
15
16
17
18 crystal (4.5 GPa) is in line with values observed for other molecular crystalline solids.^{28,}
19
20
21 ⁴⁰⁻⁴¹ Surprisingly, the Young's modulus of the **DAE** nanowire crystal (1.4 GPa) shows a
22
23
24 remarkable over threefold reduction compared to the macro-crystal. Previous studies
25
26
27
28 have also reported differences in the Young's modulus between macro- and nano-
29
30
31 dimensional solids.^{28-29, 40, 42} While the exact origin of the size-dependent mechanical
32
33
34
35 response is unknown, it likely originates from a combination of factors including
36
37
38 morphological differences, a decrease in the number of repeat units, and the increasing
39
40
41
42 contribution of surface effects (e.g. surface defects, surface energy effects) as the
43
44
45 surface-to-volume ratio increases at the nanoscale.^{28, 42-44}
46
47
48
49
50
51
52
53
54
55
56
57
58
59
60

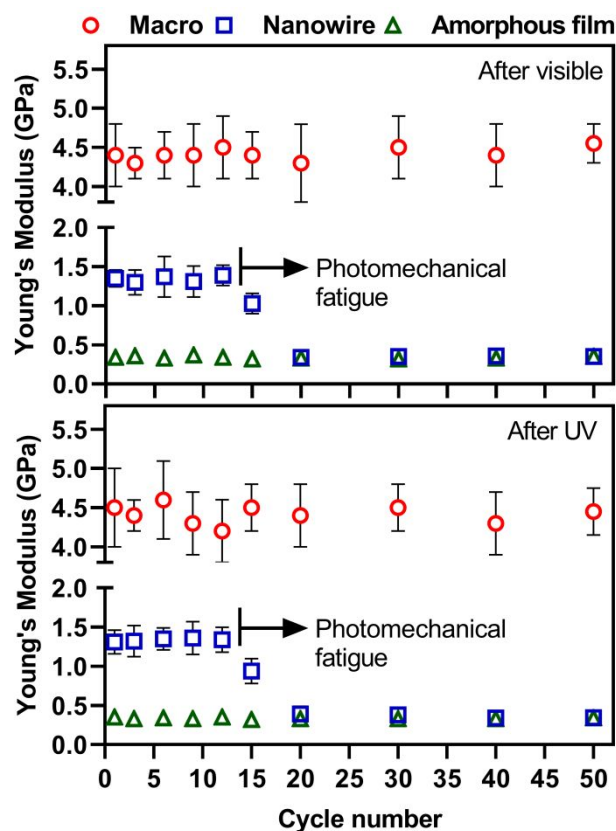


Figure 3. Young's modulus as a function of an increasing number of visible and UV light exposure cycles for a **DAE** macro crystal (red circles), nanowire (blue squares), and amorphous film (green triangles). For both macro crystal and amorphous film samples, the Young's moduli do not change over 50 light exposure cycles. The nanowire sample shows evidence of photomechanical fatigue where Young's modulus starts to decrease after 12 cycles and becomes equal to the Young's modulus of the amorphous film after

1
2
3
4 20 cycles. Subsequent light exposures up to 50 cycles do not change the nanowire elastic
5
6
7 modulus.
8
9

10
11
12
13
14 Next, the **DAE** macro-crystal, nanowire and amorphous film were repeatedly irradiated
15
16
17 with cycles of visible and UV light exposures up to a total of 50 cycles. For each solid,
18
19
20 Young's modulus was measured after every three cycles until 15th cycle, and every 10
21
22
23 cycles after the 20th cycle. Figure 3 shows the change in the Young's modulus as a
24
25
26
27 function of light exposure cycles for each solid. The Young's modulus of the macro-crystal
28
29
30 does not change over 50 light exposure cycles. This is consistent with previous reports
31
32
33 that **DAE** macro-crystals can undergo hundreds of repeated cycles of photo induced
34
35
36 bending without evidence of photomechanical fatigue.^{20, 45} The Young's modulus of **DAE**
37
38
39 amorphous film also does not change over 50 cycles of light exposures.
40
41
42
43
44

45
46 Notably, individual **DAE** nanowires showed a rapid decrease in the Young's modulus
47
48
49 from 1.4 GPa to 1.0 GPa between the 12th and 15th cycle (Figure 3). After 20 cycles, the
50
51
52 Young's modulus of the **DAE** nanowire (0.34 GPa) converges to that of the amorphous
53
54
55
56
57
58
59
60

1
2
3 film (0.35 GPa). No further changes in the modulus were observed after up to 50 cycles.
4
5

6
7 The decrease of the Young's modulus was uniform across the nanowire. The change in
8
9
10 the nanowire elastic modulus is accompanied by the appearance of hysteresis between
11
12
13 the approach and retract force data (Figure 4a), which is similar to that observed for the
14
15
16 amorphous film (see SI) and indicative of an increasing contribution of viscoelastic
17
18
19 effects.⁴⁶⁻⁴⁸ The decrease in Young's modulus and appearance of the hysteresis are clear
20
21
22
23
24 signatures of photomechanical fatigue.
25
26
27
28
29
30
31
32
33
34
35
36
37
38
39
40
41
42
43
44
45
46
47
48
49
50
51
52
53
54
55
56
57
58
59
60

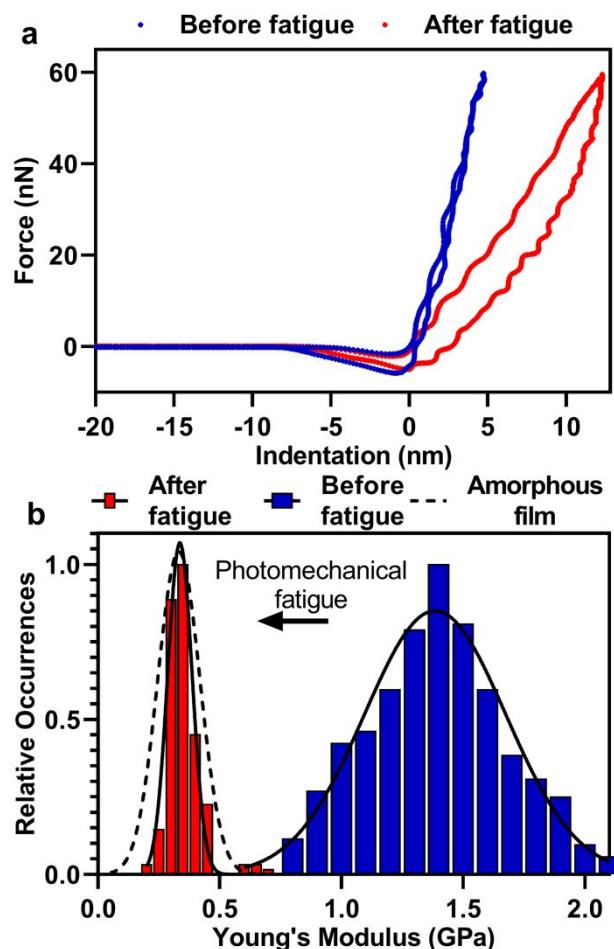
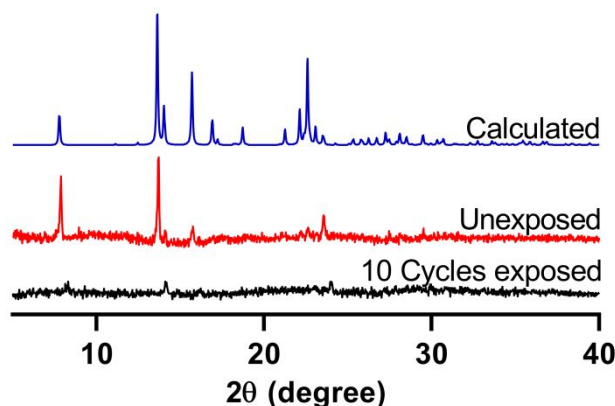


Figure 4. (a) Representative force curves (both approach and retract) collected on **DAE** nanowire before (blue) and after (red) photomechanical fatigue showing appearance of the hysteresis between the approach and retract data. (b) Histograms of Young's moduli for the **DAE** nanowire before (blue) and after (red) photomechanical fatigue. Solid black lines are Gaussian fits. The dashed black line is the Gaussian fit for Young's modulus data of amorphous film.

1
2
3
4
5
6
7 The transition in Young's modulus values for the DAE nanowires due to
8
9
10 photomechanical fatigue can be seen clearly in Figure 4b. Specifically, the fatigue results
11
12
13 in fourfold reduction of the nanowire Young's modulus (1.4 ± 0.3 GPa to 0.34 ± 0.05 GPa)
14
15
16 and overlaps with the elastic response of the amorphous film (0.35 ± 0.09 GPa).
17
18
19
20
21 Additionally, the full width at half maximum (FWHM) of the nanowire Young's moduli
22
23
24 distribution after the fatigue decreases from 0.7 GPa to 0.1 GPa, which is comparable to
25
26
27 the FWHM of 0.2 GPa for the amorphous film. The significantly narrower distributions of
28
29
30
31 elastic moduli for the fatigued nanowire and amorphous film are consistent with more
32
33
34 homogeneous mechanical response expected for an amorphous solid.⁴⁹
35
36
37

38 Because the fatigued nanowire and amorphous film both exhibit similar Young's
39
40
41 modulus values with comparable distributions and similar viscoelastic hysteresis, we
42
43
44 attribute the underlying mechanism of the photomechanical fatigue to a physical
45
46
47 transformation from the crystalline to amorphous state. To further validate this hypothesis,
48
49
50
51
52 PXR data were collected for nanowires laying horizontally on AAO template before and
53
54
55
56
57
58
59
60

1
2
3 after 10 cycles of visible and UV light exposure (Figure 5). A clear decrease (ca 90%) in
4
5
6
7 the peak intensities is evident after the repeated light exposures, consistent with our
8
9
10 hypothesis for the loss of nanowire crystallinity due to a crystalline to amorphous physical
11
12
13 transformation. We note relatively weak PXRD data is due to a quite small amount of
14
15
16
17
18 nanowire sample used for the measurements in order to ensure sufficient UV light
19
20
21 penetration into the solid to maximize conversion efficiency from **1a** to **1b**.
22
23
24
25
26
27



43 **Figure 5.** Comparison of DAE nanowires PXRD patterns: simulated pattern (blue),
44
45
46 nanowires prior to light exposure (red) and nanowires after 10 cycles of light exposure
47
48
49 (black). Significant decrease in the peak intensities as a result of light exposures supports
50
51
52 crystalline to amorphous transformation as a result of photomechanical fatigue.
53
54
55
56
57
58
59
60

1
2
3
4
5
6
7 Dong *et al.* previously reported that **DAE** nanowires embedded into AAO template
8
9
10 displayed a steady decrease in photo actuated displacement. They attributed this
11
12
13 photomechanical fatigue to a chemical reaction between **DAE** nanowires and AAO
14
15
16 template walls.²⁵ Although the **DAE** derivative used in our experiments has additional
17
18
19 methyl groups on the thiophene rings, its photochemistry is expected to be very similar.
20
21
22
23
24 Our AFM results on isolated nanowires strongly suggest that photomechanical fatigue
25
26
27
28 can result from changes in crystallinity during multiple repeated photoisomerizations. One
29
30
31 possible mechanism for the photomechanical fatigue is that an increasing number of
32
33
34
35 surface defects can nucleate and facilitate a crystalline to amorphous transformation.
36
37
38
39 Alternatively, it is possible that chemical side products can also act as defects that
40
41
42
43 nucleate this transition, with the nanowires being much more susceptible. While the exact
44
45
46 mechanism remains to be confirmed, this study provides first experimental evidence that
47
48
49 photomechanical fatigue can be dramatically accelerated in nanocrystals due to a
50
51
52
53 crystalline to amorphous physical transformation. This result suggests that the intrinsic
54
55
56
57
58
59
60

1
2
3
4 mechanical properties of bulk macro-crystals may not provide a valid foundation for the
5
6
7 design of ultrasmall photomechanical crystals or composites, since both the static
8
9
10 (Young's modulus) and dynamic (fatigue resistance) mechanical properties can be very
11
12
13
14 different for nanoscale crystals.
15
16
17
18
19
20

21 CONCLUSION

22
23
24
25
26 In summary, AFM nanoindentation was utilized to quantify changes in elastic modulus
27
28
29 (Young's modulus) of single macro-crystals, single crystal nanowires and amorphous
30
31
32
33 films composed of photochromic **DAE** molecules. The mechanical properties depend on
34
35
36
37 crystal morphology, with **DAE** nanowire crystals displaying a threefold decrease in the
38
39
40 Young's modulus compared to macro-crystals. Furthermore, while the Young's modulus
41
42
43 values for macro-crystals and amorphous film remain constant over at least 50 light
44
45
46
47 exposure cycles, the nanowires exhibit a dramatic decrease in the Young's modulus after
48
49
50 10-20 cycles. This accelerated photomechanical fatigue is attributed to a loss in
51
52
53
54 crystallinity of the nanowire.
55
56
57
58
59
60

1
2
3
4
5
6
7 **ASSOCIATED CONTENT**
8
9

10
11 **Supporting Information.** Full experimental details including materials, methods,
12
13
14
15 synthesis, and analysis along with characterization data from atomic force microscopy,
16
17
18 optical microscopy and powder X-ray diffraction.
19

20
21
22 The following files are available free of charge.
23

24
25
26 Supporting information (PDF)
27
28
29
30
31
32

33 **AUTHOR INFORMATION**
34
35
36

37 **Corresponding Author**
38
39

40
41 *E-mail: christopher.bardeen@ucr.edu
42
43

44
45 *E-mail: alexei-tivanski@uiowa.edu
46
47

48
49 **Author Contributions**
50
51
52
53
54
55
56
57
58
59
60

1
2
3
4 The manuscript was written through contributions of all authors. All authors have given
5
6
7 approval to the final version of the manuscript.
8
9

10 11 Funding Sources

12
13
14 TIL was partially supported by a University of Iowa Graduate College Summer Fellowship.

15
16
17
18 CJB and FT acknowledge financial support from the National Science Foundation grant
19
20
21 DMR-1810514 and by the MURI on Photomechanical Materials Systems (ONR N00014-
22
23
24
25 18-1-2624).
26
27

28 29 Notes

30
31
32
33 The authors declare no competing financial interest.
34
35
36
37

38 39 ABBREVIATIONS

40
41
42 AFM, atomic force microscopy; PXRD, powder x-ray diffraction.
43
44
45
46
47

48 49 REFERENCES

- 50
51
52 1. Kitagawa, D.; Kobatake, S., Crystal Thickness Dependence of Photoinduced Crystal
53 Bending of 1,2-Bis(2-methyl-5-(4-(1-naphthoyloxymethyl)phenyl)-3-
54 thienyl)perfluorocyclopentene. *J Phys Chem C* **2013**, *117* (40), 20887-20892.
55
56
57
58
59
60

2. Nath, N. K.; Pejov, L.; Nichols, S. M.; Hu, C. H.; Saleh, N.; Kahr, B.; Naumov, P., Model for Photoinduced Bending of Slender Molecular Crystals. *J Am Chem Soc* **2014**, *136* (7), 2757-2766.
3. Koshima, H.; Ojima, N.; Uchimoto, H., Mechanical Motion of Azobenzene Crystals upon Photoirradiation. *Journal of the American Chemical Society* **2009**, *131* (20), 6890-6891.
4. Kitagawa, D.; Nishi, H.; Kobatake, S., Photoinduced Twisting of a Photochromic Diarylethene Crystal. *Angew Chem Int Edit* **2013**, *52* (35), 9320-9322.
5. Al-Kaysi, R. O.; Muller, A. M.; Bardeen, C. J., Photochemically driven shape changes of crystalline organic nanorods. *J Am Chem Soc* **2006**, *128* (50), 15938-15939.
6. Kobatake, S.; Takami, S.; Muto, H.; Ishikawa, T.; Irie, M., Rapid and reversible shape changes of molecular crystals on photoirradiation. *Nature* **2007**, *446* (7137), 778-781.
7. Kitagawa, D.; Okuyama, T.; Tanaka, R.; Kobatake, S., Photoinduced Rapid and Explosive Fragmentation of Diarylethene Crystals Having Urethane Bonding. *Chem Mater* **2016**, *28* (14), 4889-4892.
8. Wang, H. R.; Chen, P.; Wu, Z.; Zhao, J. Y.; Sun, J. B.; Lu, R., Bending, Curling, Rolling, and Salient Behavior of Molecular Crystals Driven by [2+2] Cycloaddition of a Styrylbenzoxazole Derivative. *Angew Chem Int Edit* **2017**, *56* (32), 9463-9467.
9. Bushuyev, O. S.; Singleton, T. A.; Barrett, C. J., Fast, Reversible, and General Photomechanical Motion in Single Crystals of Various Azo Compounds Using Visible Light. *Adv Mater* **2013**, *25* (12), 1796-1800.
10. Bushuyev, O. S.; Tomberg, A.; Friscic, T.; Barrett, C. J., Shaping Crystals with Light: Crystal-to-Crystal Isomerization and Photomechanical Effect in Fluorinated Azobenzenes. *J Am Chem Soc* **2013**, *135* (34), 12556-12559.
11. Naumov, P.; Kowalik, J.; Solntsev, K. M.; Baldrige, A.; Moon, J. S.; Kranz, C.; Tolbert, L. M., Topochemistry and Photomechanical Effects in Crystals of Green Fluorescent Protein-like Chromophores: Effects of Hydrogen Bonding and Crystal Packing. *J Am Chem Soc* **2010**, *132* (16), 5845-5857.
12. Zhu, L. Y.; Al-Kaysi, R. O.; Bardeen, C. J., Reversible Photoinduced Twisting of Molecular Crystal Microribbons. *J Am Chem Soc* **2011**, *133* (32), 12569-12575.
13. Naumov, P.; Sahoo, S. C.; Zakharov, B. A.; Boldyreva, E. V., Dynamic Single Crystals: Kinematic Analysis of Photoinduced Crystal Jumping (The Photosalient Effect). *Angew Chem Int Edit* **2013**, *52* (38), 9990-9995.
14. Kitagawa, D.; Kobatake, S., Photoreversible current ON/OFF switching by the photoinduced bending of gold-coated diarylethene crystals. *Chem Commun* **2015**, *51* (21), 4421-4424.
15. Kitagawa, D.; Tanaka, R.; Kobatake, S., Photoinduced stepwise bending behavior of photochromic diarylethene crystals. *Crystengcomm* **2016**, *18* (38), 7236-7240.
16. Hirano, A.; Hashimoto, T.; Kitagawa, D.; Kono, K.; Kobatake, S., Dependence of Photoinduced Bending Behavior of Diarylethene Crystals on Ultraviolet Irradiation Power. *Cryst Growth Des* **2017**, *17* (9), 4819-4825.
17. Irie, M.; Fulcaminato, T.; Matsuda, K.; Kobatake, S., Photochromism of Diarylethene Molecules and Crystals: Memories, Switches, and Actuators. *Chem Rev* **2014**, *114* (24), 12174-12277.
18. Irie, M., Diarylethenes for memories and switches. *Chem Rev* **2000**, *100* (5), 1685-1716.
19. Patel, P. D.; Mikhailov, I. A.; Belfield, K. D.; Masunov, A. E., Theoretical Study of Photochromic Compounds, Part 2: Thermal Mechanism for Byproduct Formation and Fatigue

- 1
2
3 Resistance of Diarylethenes Used as Data Storage Materials. *Int J Quantum Chem* **2009**, *109* (15),
4 3711-3722.
- 5 20. Herder, M.; Schmidt, B. M.; Grubert, L.; Patzel, M.; Schwarz, J.; Hecht, S., Improving the
6 Fatigue Resistance of Diarylethene Switches. *J Am Chem Soc* **2015**, *137* (7), 2738-2747.
- 7 21. Irie, M.; Lifka, T.; Uchida, K.; Kobatake, S.; Shindo, Y., Fatigue resistant properties of
8 photochromic dithienylethenes: by-product formation. *Chem Commun* **1999**, (8), 747-748.
- 9 22. Terao, F.; Morimoto, M.; Irie, M., Light-Driven Molecular-Crystal Actuators: Rapid and
10 Reversible Bending of Rodlike Mixed Crystals of Diarylethene Derivatives. *Angew Chem Int Edit*
11 **2012**, *51* (4), 901-904.
- 12 23. Tong, F.; Kitagawa, D.; Dong, X. N.; Kobatake, S.; Bardeen, C. J., Photomechanical
13 motion of diarylethene molecular crystal nanowires. *Nanoscale* **2018**, *10* (7), 3393-3398.
- 14 24. Fu, Q. T.; Yan, X. D.; Li, T.; Zhang, X. Y.; He, Y.; Zhang, W. D.; Liu, Y.; Li, Y. X.; Gu,
15 Z. G., Diarylethene-based conjugated polymer networks for ultrafast photochromic films. *New J*
16 *Chem* **2019**, *43* (39), 15797-15803.
- 17 25. Dong, X. M.; Tong, F.; Hanson, K. M.; Al-Kaysi, R. O.; Kitagawa, D.; Kobatake, S.;
18 Bardeen, C. J., Hybrid Organic Inorganic Photon-Powered Actuators Based on Aligned
19 Diarylethene Nanocrystals. *Chem Mater* **2019**, *31* (3), 1016-1022.
- 20 26. Tong, F.; Liu, M. Y.; Al-Kaysi, R. O.; Bardeen, C. J., Surfactant-Enhanced
21 Photoisomerization and Photomechanical Response in Molecular Crystal Nanowires. *Langmuir*
22 **2018**, *34* (4), 1627-1634.
- 23 27. Naumov, P.; Chizhik, S.; Panda, M. K.; Nath, N. K.; Boldyreva, E., Mechanically
24 Responsive Molecular Crystals. *Chem Rev* **2015**, *115* (22), 12440-12490.
- 25 28. Rupasinghe, T. P.; Hutchins, K. M.; Bandaranayake, B. S.; Ghorai, S.; Karunatilake, C.;
26 Bucar, D. K.; Swenson, D. C.; Arnold, M. A.; MacGillivray, L. R.; Tivanski, A. V., Mechanical
27 Properties of a Series of Macro- and Nanodimensional Organic Cocrystals Correlate with Atomic
28 Polarizability. *Journal of the American Chemical Society* **2015**, *137* (40), 12768-12771.
- 29 29. Karunatilaka, C.; Bucar, D. K.; Ditzler, L. R.; Friscic, T.; Swenson, D. C.; MacGillivray,
30 L. R.; Tivanski, A. V., Softening and Hardening of Macro- and Nano-Sized Organic Cocrystals in
31 a Single-Crystal Transformation. *Angew Chem Int Edit* **2011**, *50* (37), 8642-8646.
- 32 30. Hutchins, K. M.; Rupasinghe, T. P.; Ditzler, L. R.; Swenson, D. C.; Sander, J. R. G.;
33 Baltrusaitis, J.; Tivanski, A. V.; MacGillivray, L. R., Nanocrystals of a Metal-Organic Complex
34 Exhibit Remarkably High Conductivity that Increases in a Single-Crystal-to-Single-Crystal
35 Transformation. *J Am Chem Soc* **2014**, *136* (19), 6778-6781.
- 36 31. Root, S. E.; Savagatrup, S.; Printz, A. D.; Rodriguez, D.; Lipomi, D. J., Mechanical
37 Properties of Organic Semiconductors for Stretchable, Highly Flexible, and Mechanically Robust
38 Electronics. *Chem Rev* **2017**, *117* (9), 6467-6499.
- 39 32. Chibani, S.; Coudert, F. X., Systematic exploration of the mechanical properties of 13 621
40 inorganic compounds. *Chemical Science* **2019**, *10* (37), 8589-8599.
- 41 33. Zhu, L. Y.; Tong, F.; Salinas, C.; Al-Muhanna, M. K.; Tham, F. S.; Kisailus, D.; Al-Kaysi,
42 R. O.; Bardeen, C. J., Improved Solid-State Photomechanical Materials by Fluorine Substitution
43 of 9-Anthracene Carboxylic Acid. *Chem Mater* **2014**, *26* (20), 6007-6015.
- 44 34. Almadori, Y.; Moerman, D.; Martinez, J. L.; Leclere, P.; Grevin, B., Multimodal
45 noncontact atomic force microscopy and Kelvin probe force microscopy investigations of
46 organolead tribromide perovskite single crystals. *Beilstein J Nanotech* **2018**, *9*, 1695-1704.
- 47
48
49
50
51
52
53
54
55
56
57
58
59
60

- 1
2
3 35. Yamada, T.; Muto, K.; Kobatake, S.; Irie, M., Crystal structure-reactivity correlation in
4 single-crystalline photochromism of 1,2-bis(2-methyl-5-phenyl-3-thienyl)perfluorocyclopentene.
5 *J Org Chem* **2001**, *66* (18), 6164-6168.
- 6 36. Tsujioka, T.; Kume, M.; Irie, M., Photochromic reactions of a diarylethene derivative in
7 polymer matrices. *J Photoch Photobio A* **1997**, *104* (1-3), 203-206.
- 8 37. Kim, M.; Yun, J. H.; Cho, M., Light penetration-coupled photoisomerization modeling for
9 photodeformation of diarylethene single crystal: upscaling isomerization to macroscopic
10 deformation. *Sci Rep-Uk* **2017**, *7*.
- 11 38. Sumi, T.; Takagi, Y.; Yagi, A.; Morimoto, M.; Irie, M., Photoirradiation wavelength
12 dependence of cycloreversion quantum yields of diarylethenes. *Chemical Communications* **2014**,
13 *50* (30), 3928-3930.
- 14 39. Jee, A. Y.; Lee, M., Comparative analysis on the nanoindentation of polymers using atomic
15 force microscopy. *Polym Test* **2010**, *29* (1), 95-99.
- 16 40. Hutchins, K. M.; Rupasinghe, T. P.; Oburn, S. M.; Ray, K. K.; Tivanski, A. V.;
17 MacGillivray, L. R., Remarkable decrease in stiffness of aspirin crystals upon reducing crystal size
18 to nanoscale dimensions via sonochemistry. *Crystengcomm* **2019**, *21* (13), 2049-2052.
- 19 41. Ohshima, S.; Morimoto, M.; Irie, M., Light-driven bending of diarylethene mixed crystals.
20 *Chem Sci* **2015**, *6* (10), 5746-5752.
- 21 42. Tiba, A.; Tivanski, A. V.; MacGillivray, L. R., Size-Dependent Mechanical Properties of
22 a Metal-Organic Framework: Increase in Flexibility of ZIF-8 by Crystal Downsizing. *Nano Lett*
23 **2019**, *19* (9), 6140-6143.
- 24 43. Huxter, V. M.; Lee, A.; Lo, S. S.; Scholes, G. D., CdSe Nanoparticle Elasticity and Surface
25 Energy. *Nano Letters* **2009**, *9* (1), 405-409.
- 26 44. Xu, W. W.; Davila, L. P., Size dependence of elastic mechanical properties of
27 nanocrystalline aluminum. *Mat Sci Eng a-Struct* **2017**, *692*, 90-94.
- 28 45. Morimoto, M.; Irie, M., A Diarylethene Cocrystal that Converts Light into Mechanical
29 Work. *J Am Chem Soc* **2010**, *132* (40), 14172-14178.
- 30 46. Ray, K. K.; Lee, H. D.; Gutierrez, M. A.; Chang, F. J.; Tivanski, A. V., Correlating 3D
31 Morphology, Phase State, and Viscoelastic Properties of Individual Substrate-Deposited Particles.
32 *Anal Chem* **2019**, *91* (12), 7621-7630.
- 33 47. Lee, H. D.; Ray, K. K.; Tivanski, A. V., Solid, Semisolid, and Liquid Phase States of
34 Individual Submicrometer Particles Directly Probed Using Atomic Force Microscopy. *Anal Chem*
35 **2017**, *89* (23), 12720-12726.
- 36 48. Bremmell, K. E.; Evans, A.; Prestidge, C. A., Deformation and nano-rheology of red blood
37 cells: An AFM investigation. *Colloid Surface B* **2006**, *50* (1), 43-48.
- 38 49. Ward, S.; Perkins, M.; Zhang, J. X.; Roberts, C. J.; Madden, C. E.; Luk, S. Y.; Patel, N.;
39 Ebbens, S. J., Identifying and mapping surface amorphous domains. *Pharm Res-Dordr* **2005**, *22*
40 (7), 1195-1202.
- 41
42
43
44
45
46
47
48
49
50
51
52
53
54
55
56
57
58
59
60

Use of TOC only:

